Flux-periodicity crossover from *h/2e* to *h/e* in aluminium nano-loops

IOP Conf. Series: Journal of Physics: Conf. Series **969** (2018) 012063 doi:10.1088/1742-6596/969/1/012063

Flux-periodicity crossover from *h/2e* to *h/e* in aluminium nano-loops

C. Espy[1], O. J. Sharon[2], J. Braun[1], R. Garreis[1], F. Strigl[1], A. Shaulov[2], P. Leiderer[1], E. Scheer[1,*], Y. Yeshurun[2]

[1]Department of Physics, University of Konstanz, 78457 Konstanz, Germany
[2]Department of Physics and Institute of Nano Technology and Advanced Materials, Bar-Ilan University, 5290002 Ramat-Gan, Israel
*Elke.scheer@uni-konstanz.de

Abstract. We study the magnetoresistance of aluminium 'double-networks' formed by connecting the vertexes of nano-loops with relatively long wires, creating two interlaced subnetworks of small and large loops (SL and LL, respectively). Far below the critical temperature, Aharonov-Bohm like quantum interference effects are observed for both the LL and the SL subnetworks. When approaching T_c, both exhibit the usual Little-Parks oscillations, with periodicity of the superconducting flux quantum $\Phi_0=h/2e$. For one sample, with a relatively large coherence length, ξ, at temperatures very close to T_c, the Φ_0 periodicity of the SL disappears, and the waveform of the first period is consistent with that predicted recently for loops with a size $a < \xi$, indicating a crossover to $2\Phi_0$ periodicity.

1. Introduction

In a multiply connected superconductor, the fluxoid, defined as the sum of the magnetic flux and the line integral of the screening current, is quantized in units of $\Phi_0 = h/2e$, where the *2e* is a hallmark of electron pairing in the superconductor. As a direct consequence of this fluxoid quantization, periodic oscillations of the critical temperature T_c as a function of magnetic field, known as the Little-Parks effect manifest themselves as oscillations of the magnetoresistance (MR) close to T_c. The amplitudes of the critical temperature, ΔT_c, and the magnetoresistance oscillations, ΔR, are related by the slope of the resistance *vs.* temperature, $R(T)$: $\Delta R \approx (\mathrm{d}R/\mathrm{d}T)\Delta T_c$ [1].

Theoretical studies [2] have predicted that in superconducting nano-loops with a length-scale $a < \xi$ the dominant periodicity is *h*/*e* rather than *h*/2*e*. The same theories predict that for high-T_c superconductors (HTS) with d-wave symmetry, the *h*/*e* periodicity is also expected for $a \gtrsim \xi$. Recent experiments ([3, 4]) failed to identify the *h*/*e* component in HTS, probably because ξ_0 in these materials is only ~2 nm and, therefore, $a >> \xi$ in most of the temperature range.

In the present study we focus on aluminium, a low-T_c superconductor with a relatively large bulk coherence length (ξ_0 = 1.6 μm). In nanostructures made of diffusive thin films the coherence length is reduced due to the finite mean free path, and simultaneously the penetration depth λ_L is enhanced. Typical values of ξ in these aluminium nanostructures lie in the range of 100 to 200 nm. Close to T_c, the coherence length $\xi(T)$ diverges, allowing in principle to meet the criterion $a < \xi$ in nanostructures with circumferences in the order of several hundred nanometres. On the other hand, the critical field of

bulk Al amounts to only 10 mT, giving a strong limitation for the number of Little-Parks oscillations (LPO) that can be observed. In reduced dimension, *i.e.* when the lateral dimensions are in the order of the penetration depth λ_L, the critical field B_c may increase to a few hundred mT. Taking these considerations together, we fabricated 'double-networks' [3], see figure 1, with small loops of order of 400 x 400 nm^2, connected by wires of ~ 1600 nm length. An applied field of ~ 10 mT corresponds to a flux of $h/2e$ through the small loops.

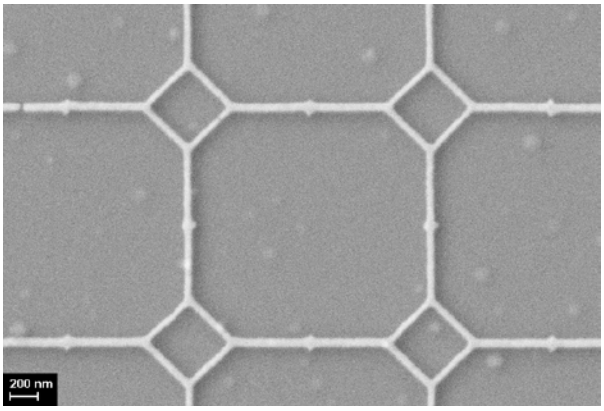

Figure 1. Scanning electron micrograph of an Al double-network (sample 1) with large (small) loop side length 1.71 µm (426 nm), line width $w = 50 \pm 5$ nm, thickness $d = 30$ nm.

2. Experimental

2.1. Sample fabrication

We use a lift-off electron beam lithography process in which Al is electron-beam evaporated onto a cooled, pre-patterned, oxidized Si substrate. The lithographic mask is then removed in warm acetone. The width of the lines is around 60 nm, the film thickness amounts to 30 nm. The arrays consist of roughly 10 x 10 loops. The samples feature normal state resistance of $R_n = 20$ - 40 Ω.

2.2. Transport measurements

Due to the pronounced temperature dependence of the LPO, particular care is taken to stabilize the cryostat temperature during the magnetic field sweeps. We use a combination of a carefully calibrated resistive thermometer to determine the absolute temperature and a capacitive sensor for keeping it constant within ± 1 mK around the set-point temperature. The set temperature spacing is adapted to the steepness of the $R(T)$ curves and amounts to a few mK around T_c. Before starting the magnetoresistance sweeps the temperature is allowed to stabilize for several minutes.

The cryostat is equipped with home-made high-frequency filtered cables to record the four-point differential resistance dV/dI by biasing a DC bias current that is kept smaller than 500 nA superimposed with a small AC current in lock-in technique. We simultaneously measured the resistance $R = V/I$ which shows qualitatively the same but more noisy data than the dV/dI. The low temperature critical current of the samples amounts to 50 - 250 µA. Close to T_c, where the LPO are maximal, the zero-field critical current still amounts to more than 2 µA.

The magnetic field is applied perpendicular to the sample plane using a superconducting solenoid. For each temperature, measurements are performed at a sweep rate of ~ 5 mT/min. For each temperature we record a sweep with increasing and decreasing field, as a control for constant temperature throughout a sweep, and in order to be able to correct for small field offsets. The field range is adapted to the critical field at the set temperature.

Table 1. Dimensions and transport characteristics of the two samples presented in this article. LL: large loops, SL small loops. w: line width from electron micrographs, w_{fit}: line width from fit to eq. (1), ξ: coherence length from fit to eq. (1), ξ_{cal}: coherence length from fit to eq. (2), T_c: critical temperature, I_c: critical current at 300 mK, B_c: critical field extrapolated to T = 0 from the dV/dI(B) measurements, R_n: normal resistance measured above B_c. For sample 2 the fits have been performed with the low-bias data shown in figure 3.

Sample No.	SL size (nm)	LL size (nm)	w (nm)	w_{fit} (nm)	ξ_{cal} (nm)	ξ (nm)	T_c (mK)	I_c (μA)	B_c (mT)	R_n (Ω)
1	426±10	1710±30	50±10	50±5	118±24	102±10	1408±5	55±5	194±10	33.2±1
2	324±10	1540±30	66±10	61±5	114±19	137±15	1457±5	240±10	152±10	23.3±1

3. Results

3.1. Critical temperature, critical field and coherence length

Figure 2 a) shows differential MR, dV/dI(B), curves in the temperature range 380 - 1600 mK, recorded on sample 1 with 426 nm side length of the small loops and 1.71 μm of the large loops (see table 1 for sample dimensions). From the set of dV/dI(B) curves we construct the envelope of the $B_c(T)$ phase boundary (without the oscillatory part) from which we deduce the coherence length, ξ, and T_c using the relation [7]

$$T_c(B) = T_c\left[1 - \frac{\pi^2}{3}\left(\frac{w_{fit}\xi B}{\Phi_0}\right)^2\right], \qquad (1)$$

where $\boldsymbol{w_{fit}}$ is the width of the wire. For comparison we also estimate the coherence length from the low temperature critical field, $B_c(0)$ assuming a thin slab in magnetic field resulting in the relation [10]:

$$\xi_{cal} = \sqrt{3}\Phi_0/(\pi w B_c(0)) \qquad (2)$$

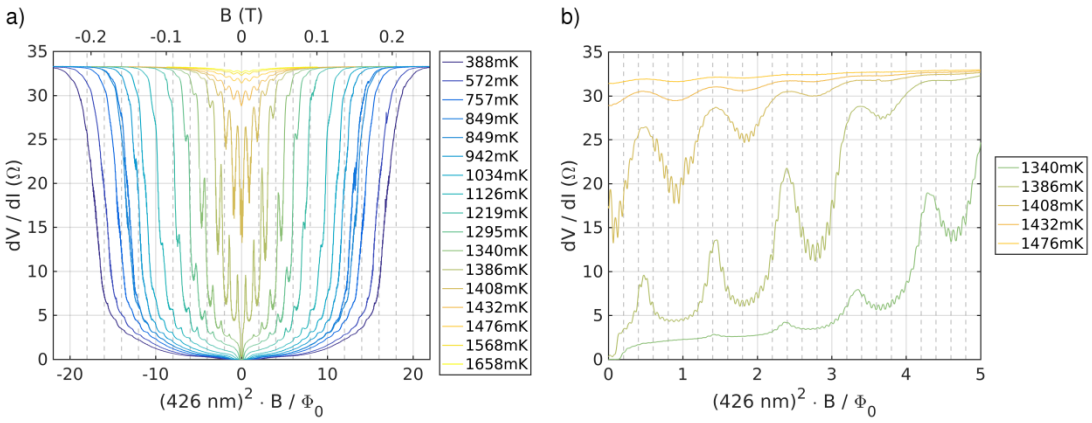

Figure 2. a) dV/dI(B) curves of sample 1 covering the whole field range and the whole temperature range from 388 mK (dark blue) to 1658 mK (yellow), b) Zoom into the positive field direction of selected data from panel a) close to T_c.

The loop sizes have been determined by inspection of the electron micrographs and are additionally deduced from the observed flux periodicity assuming square-shaped loops. The numerical values for the various parameters are given in table 1. The values for T_c correspond well with the position of the $R(T) = R_n/2$ in the temperature curves as well as with the dV/dI(B) curve at which the largest oscillation amplitude is observed. Also, both estimates for the coherence length agree with each other

within ~ 20% for both samples, supporting the suitability of the simplified models. Taking the average value of these two estimates, we find that for sample 1 (2) the ratio between the coherence length and the SL edge length a amounts to $\xi/a \sim 0.26$ (0.39). Thus, we expect the transition to the h/e periodicity being more likely to be observable in sample 2.

3.2. Little Parks effect

Figure 2 b) zooms into the positive field direction close to T_c. Figure 3 shows dV/dI(B) data for sample 2 with SL size of 324 nm and LL size of 1.54 µm. For both samples and at all temperatures we observe symmetric periodic oscillations of dV/dI(B) corresponding to $h/2e$ oscillations of the small loops (SL) and of the large loops (LL).

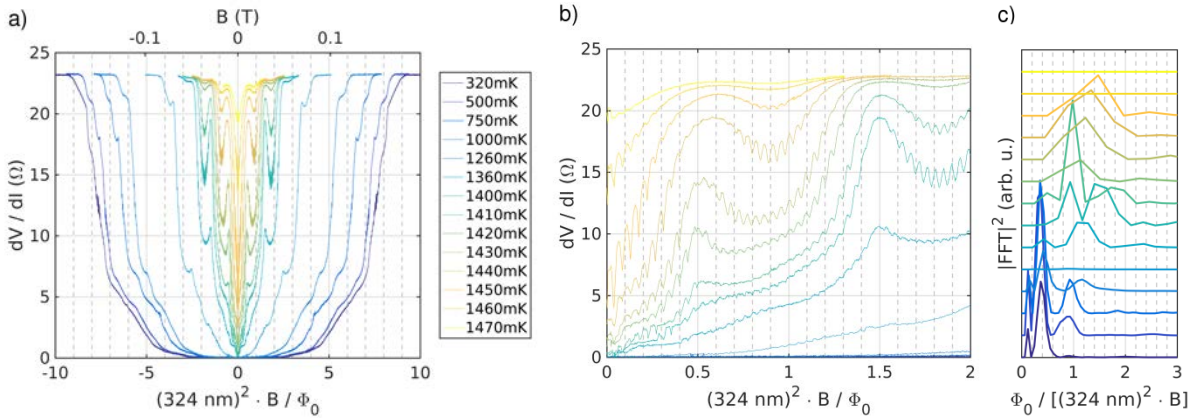

Figure 3. a) Selected dV/dI(B) traces of sample 2. b) Same curves as in a) for a reduced range in positive field direction. c) FFT of the dV/dI(B) data shown in a).

Closer inspection reveals for both samples a gradual change of the LL oscillations from a cusp-up form (typical of LPO) at low temperature, through a sinusoidal behaviour at intermediate temperature, into a cusp-down (SQUID-like) shape at higher temperatures. A similar crossover, induced by the bias current rather than by temperature, was reported by Sharon *et al.* for Nb chains of rings [5]. The effect is most pronounced at low fields when the flux through the SL is still smaller than $\Phi_0/2$. The amplitude of the LL oscillations vanishes at somewhat smaller temperatures than the SL oscillations. Both observations suggest that the coherence in the LLs is not fully developed and that weak links exist that act as Josephson junctions. Furthermore the amplitude of the LL oscillations is locally suppressed at odd multiples of $\Phi_0/2$ of the SLs. At these flux values the ring current in the SL is maximal. Hence, the suppression of the LL amplitude can be understood as an interruption of the ring current in the LLs. Similar observations were made in Al nanostructures consisting of several loops sharing the same strands [6, 7]. This observation is related to the Little-Parks-de Gennes effect [8] which describes the destruction and restauration of superconductivity in multiply connected superconductors around odd multiples of $\Phi_0/2$ [9].

3.3. Little-Parks effect of small loops and transition to h/e periodicity

We now turn to discuss the SL oscillations. These also show the typical cusp-up behaviour well below T_c and a sinusoidal shape close to T_c. This shape transition is most pronounced in sample 2 and is marked by a broadening and a shift of the resistance maximum at $\Phi_0/2$ to larger fields. The Fast Fourier Transform (FFT) of the data (see figure 3 c)) reveals that besides the usual $h/2e$ component also an $h/3e$ component is present which starts to dominate close to T_c. The $h/3e$ component indicates a modulation of the amplitude of the regular $h/2e$ LPO. We interpret these findings as an onset of the transition to h/e which is expected for very small loop sizes. Due to the limited field range that covers

only slightly more than one period of the *h*/*e*, the fundamental *h*/*e* component cannot be seen in the FFT, but rather a higher harmonic of it, *i.e.* the *h*/3*e* component.

To investigate this observation further we performed d*V*/d*I*(*B*) measurements on sample 2 under relatively high bias current of 2.1 µA. With this bias the apparent T_c is somewhat smaller than in the low bias data. Two examples of differential resistance curves, one with low and one with high bias, are plotted in figure 4 a). In the high-bias data the oscillations appear more pronounced and d*V*/d*I*(*B*) exceeds R_n around $\Phi = \Phi_0/2$ and close to B_c(T). In these field ranges also irregular oscillations are visible although the LPOs are washed out in the low bias data. Both observations are consequences of the non-linear current-voltage characteristics in this range and the differential measurement scheme. We checked that the absolute resistance remains everywhere smaller than R_n.

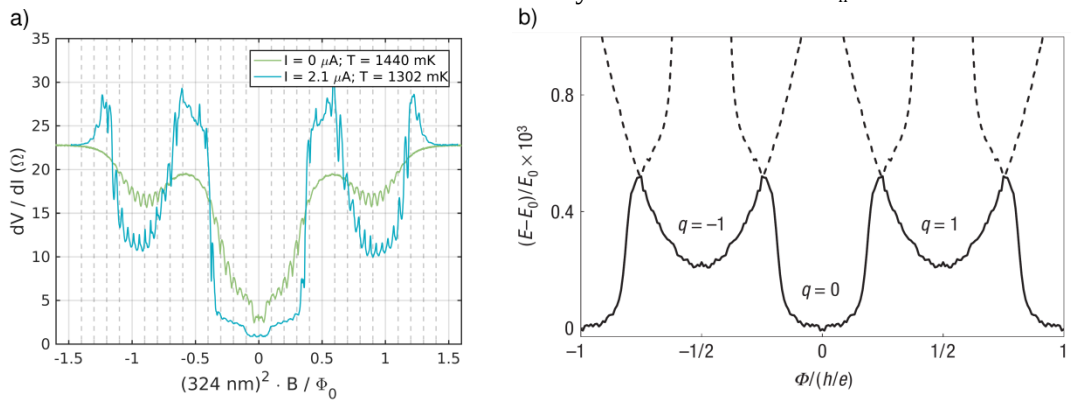

Figure 4. a) Comparison of differential resistance *vs*. *B* curves of sample 2 with zero DC bias current and with finite DC bias current (2.1 µA) close to T_c. b) Energy vs. flux for a superconducting loop with $a < \xi$, showing the modulation of the odd LPOs. Reprinted with permission from MacMillan Publishers Ltd: Nature Physics [2], copyright 2008. In this right figure Φ is described in units of $\Phi_0 = h/e$.

For both curves, the shape of the central dip (at $\Phi = 0$) is much different from that of the side dips (at $\Phi = \Phi_0$), implying that the Little-Parks *h*/2*e* periodicity is broken. On the other hand, these data show a striking similarity to the theoretical calculations of Loder *et al.* [2] predicting *h*/*e* periodicity, as depicted in figure 4 b). Note that in this figure the flux is plotted in units of *h*/*e*. Unfortunately, we observe only one period as the field required to observe more periods exceeds the critical field, $B_c(0)$, of this sample. Nevertheless, the nearly parabolic shape of the side minima and the distorted shape of the parabola centred at $\Phi = 0$ may serve as a fingerprint of the predicted *h*/*e* periodicity. Note that the theoretical prediction (right panel) describes the oscillation in the energy while the experimental results (left) describe the differential resistance. The two, however, are related since both are directly related to ΔT_c [10]. The similarity with the theoretical curve is most apparent for the high-bias d*V*/d*I* curve. This suggests that under these measurement conditions, *i.e.* when the system is driven close to the transition to the normal state, the relation between differential resistance and energy is most direct.

3.4. Aharonov-Bohm effect in small loops

Finally we note that the temperature dependence of the amplitude of the SL oscillations is non-monotonous. As figure 3 c) shows, at low temperature, $T <$ ~1000 mK, we observe *h*/*e* and *h*/2*e* oscillations of the small loops that almost disappear for intermediate temperatures, ~1000 mK < $T <$ ~1200 mK. Above 1200 mK dominantly the *h*/2*e* and *h*/3*e* components corresponding to the Little-Parks effect appear. We attribute the low-temperature oscillations to quantum interference effects, *i.e.* the Aharonov–Bohm effect, indicating that also the phase coherence length of the quasiparticles, $L_{\Phi,}$ in this range is in the order of the perimeter of the SLs or larger. When increasing the temperature,

inelastic scattering sets in that reduces L_Φ [11]. For completeness we mention that we do not observe such non-monotonous behaviour for the LL oscillations, indicating that L_Φ is always smaller than the perimeter of the LLs.

4. Conclusions

Summarizing, we have presented magnetoresistance data in interlaced networks comprising small and large loops made of aluminium. We observe the interplay between the magnetoresistance oscillations in these two subsets of loops. In particular, the $\Phi_0 = h/2e$ periodic Little-Parks oscillations of the large loops are modulated by the flux conditions in the small loops. For a sample with high ratio between coherence length and loop size we observe an onset of the transition from the conventional $h/2e$ to an h/e periodicity, as predicted for long coherence length. A full experimental verification of the theory requires measurements of more than one period. However, the relatively low critical field of aluminium, and the large period of small loops, presently impedes achieving this condition. Further improvements of the sample design and material quality are currently underway to overcome this limitation.

Acknowledgements

This research was supported by a Grant from the GIF, the German-Israeli Foundation for Scientific Research and Development. We thank Arno Kampf, Thilo Kopp, Jochen Mannhart, and Christoph Strunk for insightful discussion and Simon Haus for his help in sample preparation.

References

[1] Little W, Parks R 1962 *Phys. Rev. Lett*. **9** 9.
[2] Loder F, Kampf A P, Kopp T, Mannhart J, Schneider, C W, Barash, Y S 2008 *Nature Phys* **4** 112.
[3] Sochnikov I, Shaulov A, Yeshurun Y, Logvenov G, Božović I 2010 *Nature Nanotechnol*. **5** 516.
[4] Carillo F, Papari G, Stornaiuolo D, Born D, Montemurro D, Pingue P, Beltram F, Tafuri F 2010 *Phys. Rev. B* **81** 054505.
[5] Sharon O J, Shaulov A, Berger J, Sharoni A, Yeshurun Y 2016 *Sci. Rep*. **6** 28320.
[6] Bruyndoncx V, Strunk C, Moshchalkov V V, van Haesendonck C, Bruynseraede Y 1996 *Europhys. Lett.* **36** 449.
[7] Strunk C, Bruyndoncx V, Moshchalkov V V, Van Haesendonck C, Bruynseraede Y Jonckheere R 1996 *Phys. Rev. B* **54** R12701.
[8] de Gennes P G, 1981 *C. R. Acad. Sci. Ser. B* **292** 9, and *ibid.* **292** 279.
[9] Staley N E, Liu Y 2012 *Proc. Nat. Acad. Sci* **109** 14819.
[10] Tinkham M 1996 *Introduction to Superconductivity* McGraw-Hill New York.
[11] Washburn S, Webb R A 1986, *Adv. Phys.* **35** 375.